INTERACTIVE LEVEL SET SEGMENTATION FOR IMAGE-GUIDED THERAPY

Nir Ben-Zadok[*1], *Tammy Riklin-Raviv*[†2], *Nahum Kiryati*[1]

[1] School of Electrical Engineering, Tel-Aviv University
[2] Department of Electrical Engineering and Computer Science, Massachusetts Institute of Technology

ABSTRACT

Image-guided therapy procedures require the patient to remain still throughout the image acquisition, data analysis and therapy. This imposes a tight time constraint on the overall process. Automatic extraction of the pathological regions prior to the therapy can be faster than the customary manual segmentation performed by the physician. However, the image data alone is usually not sufficient for reliable and unambiguous computerized segmentation. Thus, the oversight of an experienced physician remains mandatory.

We present a novel segmentation framework, that allows user feedback. A few mouse-clicks of the user, discrete in nature, are represented as a continuous energy term that is incorporated into a level-set functional. We demonstrate the proposed method on MR scans of uterine fibroids acquired prior to focused ultrasound ablation treatment. The experiments show that with a minimal user input, automatic segmentation results become practically identical to manual expert segmentation.

Index Terms— MR scans segmentation, Level-set framework, User interaction, Image guided therapy

1. INTRODUCTION

Image-guided therapy (IGT) utilizes images acquired before therapy for localization of the pathological regions to be treated. The position of the imaged region of interest (ROI) must not change throughout the IGT procedure. This requires to minimize the time lapse between image acquisition and therapy. Automatic, rather than manual, delineation of the ROI boundaries can speed up the analysis process. However, phenomena such as noise, blur and sampling artifacts caused by limitations of the acquisition modalities, make automatic segmentation challenging and not sufficiently reliable [1]. Moreover, the use of shape or intensity priors is limited due to the intricacy and variability of anatomical structures. The knowhow of an experienced physician is mandatory for fine tuning and final approval of the boundaries of the ROI to be treated.

Segmentation methods which allow user interaction are the key for fast and reliable extraction of the ROI. Current methods differ by the amount and the type of information provided by the user. Their underlying mathematical framework is a significant factor determining the form of interaction. In the *United Snakes* framework [2], based on the classical snake formulation [3], the user controls the snake evolution by 'planting' seed points. The *GrabCut* technique [4] is based on the discrete graph-cut approach, where image pixels represent graph vertices. The partitioning of the image into object and background regions is obtained by solving the min-cut problem in graphs. The user controls the segmentation by labeling regions, which are correspondingly assigned to either the source or the sink of the graph. The selected regions provide color statistics that characterize the object and the background and are utilized for segmentation. In [5] a user draws contours which are rough, cartoon-like approximations to the true boundary. The algorithm automatically learns a set of statistics from these scribbles and uses this information to segment the remainder of the image. The *live wire* technique which is based on two independent works [6, 7] uses the Dijkstra algorithm to find the shortest paths between manually-segmented segments. Distance is typically defined to be inversely related to image gradients so shortest paths follow edges in the image. Despite their popularity *live wire*, *GabCut* and similar methods that rely on the foreground color statistics or low gradient pathes are not suitable for the segmentation of medical images. Due to low contrast, noise and blurry boundaries, often the ROI cannot be distinguished from the background based on gray level statistics or edges alone, even when calculated with the user's guidance.

User interactive segmentation methods for medical image analysis include [8, 9, 10]. In [8] a semi-automatic segmentation of the left ventricle is demonstrated. The method uses linear or quadratic interpolation to convert the user input into closed structures. Hence, the feedback is not part of the level-set formulation. In [9] a method for 3D cortical segmentation that utilizes dual-front active contours and active regions is presented. The user can modify the initialization of the active region by adding or deleting labels. In [10] a probabilistic level-set method which supports user interaction is proposed.

T. Riklin Raviv and N. Ben-Zadok contributed equally to this manuscript.

T. Riklin Raviv performed the work while at Tel-Aviv University.

The authors thank Eyal Zadicario, Amit Sokolov and Gilat Schiff from InSightec Ltd. for providing the data sets and technical support. The authors thank A.M.N. foundation for the financial support.

The user-labeled input points are viewed as independent measurements of the scene.

We propose a coherent, active-contour segmentation method which supports an intuitive and friendly user interaction subject to the 'bottom up' constraints introduced by the image features. The user does not 'edit' the segmentation but influences its evolution with a few mouse clicks located in regions of 'disagreement'. This is made possible by using the level-set framework [11] which allows parametrization-free representation of the segmenting contour and automatic topology changes. The method we suggest consists of two phases. A fully automatic segmentation is first obtained by minimizing, via gradient descent, a cost functional that is based on the image data alone. The user can then provide feedback relating the initial segmentation. The user input, discrete in nature, is formulated as a continuous energy term that is incorporated into the primary cost functional. The additional term affects the gradient descent process attracting it toward a new local minimum. This results in a modified segmentation consistent with both the low-level image data and the top-down user feedback points.

The proposed method is general and can be applied to various medical image analysis tasks including image-guided therapy. We demonstrate its performances on abdomen MR scans with various forms of uterine fibroids. The segmentation is a part of a clinical procedure used to guide subsequent focused ultrasound ablation treatment. We chose a 2D slice by slice segmentation over complete 3D processing since in the given imaging set-up the off-plane resolution is significantly lower than the in-plane resolution. As is demonstrated by the examples in Section 4[1], only a few mouse clicks are needed to obtain segmentation results that are practically equivalent to expert manual segmentation. The proposed automatic-user-guided segmentation is therefore a highly reliable yet much faster alternative to the fully manual segmentation procedures currently used.

The remainder of the paper is organized as follows: In Section 2 we briefly review the state-of-the-art level set segmentation framework. In Section 3 we introduce the user feedback term. Results are shown in Section 4 followed by a discussion in Section 5.

2. LEVEL SET SEGMENTATION

Let $I\colon \Omega \rightarrow \mathbb{R}^+$ denote a gray-level image, where $\Omega \subset \mathbb{R}^2$ is the image domain. We use a level-set function ϕ to partition the image domain into two disjoint (not necessarily connected) regions corresponding to the region of interest (ROI) and the background. The ROI boundaries are represented by the zero level of ϕ: $C(t) = \{\mathbf{x}|\phi(\mathbf{x},t) = 0\}$, where $\mathbf{x} \equiv (x,y)$. Similar to [12] we use the regularized form of the Heaviside function of $\phi : \tilde{H}(\phi) = \frac{1}{2}(1 + \frac{2}{\pi}\arctan(\frac{\phi}{\epsilon}))$ to label the image regions. The scalar ϵ is hereby set to 1.

We construct a level-set segmentation functional that is composed of the classical image intensities and gradients terms, denoted by E_{MV} and E_{GAC}, respectively and the proposed user feedback term E_{USER} :

$$E(\phi) = \alpha E_{\text{MV}} + \beta E_{\text{GAC}} + \xi E_{\text{USER}}. \tag{1}$$

The weights α, β and ξ are non-negative scalars. When ξ is positive the user term influences the segmentation.

The evolution of the level set function ϕ at each iteration is determined by a gradient descent process:

$$\phi(t + \Delta t) = \phi(t) + \phi_t \Delta t, \tag{2}$$

where ϕ_t is obtained from the first variation of the cost functional (1):

$$\phi_t = \alpha\phi_t^{\text{MV}} + \beta\phi_t^{\text{GAC}} + \xi\phi_t^{\text{USER}}. \tag{3}$$

We next describe the classical terms of the functional and their associated gradient descent equations.

2.1. Region Based Term

Similar to [12] we use the minimal variance term:

$$\begin{aligned} E_{\text{MV}}(c^+, c^-, \phi) &= \int_\Omega (I - c^+)^2 \tilde{H}(\phi(\mathbf{x}))d\mathbf{x} \\ &+ \int_\Omega (I - c^-)^2 (1 - \tilde{H}(\phi(\mathbf{x})))d\mathbf{x}, \end{aligned} \tag{4}$$

where c^+ and c^- are the average intensities in the foreground and background image regions, respectively. The gradient descent equation associated with E_{MV} is:

$$\phi_t^{\text{MV}} = \tilde{\delta}(\phi)[-(I - c^+)^2 + (I - c^-)^2]. \tag{5}$$

2.2. Smoothness and Edge Based Term

We use the geodesic active contour (GAC) term as in [13, 14]:

$$E_{\text{GAC}} = \int_\Omega g_{\text{GAC}}(\mathbf{x})|\nabla\tilde{H}(\phi(\mathbf{x}))|d\mathbf{x}, \tag{6}$$

where $g_{\text{GAC}}(\mathbf{x})$ is an inverse edge-indicator function

$$g_{\text{GAC}}(\mathbf{x}) = 1/(1 + \varphi|\nabla I|^2)\ ,\ \varphi \geq 0. \tag{7}$$

E_{GAC} is minimized when the evolving contour is aligned with the local maxima of image gradients. The gradient descent equation associated with E_{GAC} is:

$$\phi_t^{\text{GAC}} = \tilde{\delta}(\phi) \cdot \text{div}(g_{\text{GAC}}(\mathbf{x}) \cdot \nabla\phi/|\nabla\phi|), \tag{8}$$

where **div** is the divergence operator. In this work, the scalar φ in eq. (7) is set to 1. Note, however, that when φ is set to zero, eq. (6) reduces to the classical smoothness term:

$$E_{\text{LEN}} = \int_\Omega |\nabla\tilde{H}(\phi(\mathbf{x}))|d\mathbf{x}. \tag{9}$$

We next introduce the user-feedback term, which is the essence of the proposed contribution.

[1] More segmentation examples, including a demonstration video, are available online at http://www.eng.tau.ac.il/~nk/ISBI09

3. USER FEEDBACK

Let $\{\mathbf{x}_i\}_{i=1}^n$ denote the set of user feedback points. We define $M\colon \Omega \to \{0,1\}$:

$$M(\mathbf{z}) = \sum_{i=1}^{n} \delta(\mathbf{z} - \mathbf{x}_i) \tag{10}$$

where $\delta(\mathbf{z})$ is the 2D Dirac delta function.

The function $L\colon \Omega \to \mathbb{R}$ represents the user feedback with respect to the final level-set function $\hat{\phi}$ of the first phase:

$$L(\mathbf{x}) = \tilde{H}(\hat{\phi}(\mathbf{x})) + \left\{1 - 2\tilde{H}(\hat{\phi}(\mathbf{x}))\right\} \int_{\mathbf{z}\in\lambda} M(\mathbf{z}) d\mathbf{z}, \tag{11}$$

where λ is an infinitesimal neighborhood of the coordinate $\mathbf{x}$. Hence, for each $\mathbf{x} \in \{\mathbf{x}_i\}_{i=1}^n$, $L(\mathbf{x}) = 0$ if the feedback point is within the segmented region of the first phase. $L(\mathbf{x}) = 1$ if the feedback point is located in the background. $L(\mathbf{x}) = \tilde{H}(\hat{\phi}(\mathbf{x}))$ if $\mathbf{x}$ is not marked.

The indicator function $L(\mathbf{x})$ is used in the formulation of the energy term which incorporates the user feedback:

$$E_{\text{USER}} = \int_{\mathbf{x}\in\Omega} \int_{\mathbf{x}'\in\Omega} \left(L(\mathbf{x}') - \tilde{H}(\phi(\mathbf{x}))\right)^2 K(\mathbf{x},\mathbf{x}') d\mathbf{x}' d\mathbf{x} \tag{12}$$

where K is a Gaussian kernel:

$$K(\mathbf{x},\mathbf{x}') = \frac{1}{2\pi|\Sigma|^{\frac{1}{2}}} \exp\left\{-\frac{(\mathbf{x}-\mathbf{x}')^T\Sigma^{-1}(\mathbf{x}-\mathbf{x}')}{2}\right\} \tag{13}$$

and Σ is the 2×2 covariance matrix.

The algorithm supports two modes of user feedback. The user may either draw a cross such that its eccentricity and orientation determines the entries of the covariance matrix Σ or can provide a point-wise mouse click, which is represented by a diagonal Σ with identical entries. The gradient descent equation associated with E_{USER} has the form:

$$\phi_t^{\text{USER}}(\mathbf{x}) = 2\tilde{\delta}(\phi) \int_{\mathbf{x}'\in\Omega} \left(L(\mathbf{x}') - \tilde{H}(\phi(\mathbf{x}))\right) K(\mathbf{x},\mathbf{x}') d\mathbf{x}'. \tag{14}$$

4. EXPERIMENTAL RESULTS

We demonstrate the proposed method by segmenting uterine fibroids in MR scans acquired by a 1.5T whole-body system (Genesis Signa; GE Medical Systems, Milwaukee, Wis.). Segmentation results are compared to the boundaries of the fibroids that were manually delineated by an experienced radiologist. Qualitative evaluation is via visual inspection. Quantitative evaluation is based on standard measures [15], the True Positive Fraction (TPF) and the False Positive Fraction (FPF). We set the parameters of the functional (1) for all scans as follows: $\alpha = 1, \beta = 1.5$ and ξ is set to 1 in the second phase to allow user interaction. For the point-wise user mode the covariance matrix Σ corresponds to an isotropic Gaussian with a standard deviation of 3. Fig. 1 shows segmentations of uterine fibroids in abdomen MR scans of different patients prior to the user interaction and afterwards. User feedback points are placed both inside and outside the preliminary segmented regions. The last row of Fig. 1 exemplifies the user 'cross mode'. The boundaries drawn by the expert are shown in red. Quantitative comparisons of the segmentations shown in Fig. 1 with the respective manual expert segmentations are presented in Table 1. More examples, including a demonstration video, are available online at [16].

Table 1. True Positive Fraction (TPF) and False Positive Fraction (FPF) of the segmentation obtained before (Phase 1) and after (Phase 2) user feedback. Additional comparisons are available online [16].

Patient, Slice	TPF		FPF	
	Phase 1	Phase 2	Phase 1	Phase 2
A, 3	0.9976	0.9985	0.0056	0.0005
B, 6	0.9641	1.0000	0.0044	0.0024
C, 5	0.9749	0.9983	0.0000	0.0007
D, 5$^\sharp$	0.9810	0.9926	0.0204	0.0150

$^\sharp$Cross-sign feedback

5. SUMMARY AND FUTURE DIRECTIONS

Image-guided therapy (IGT) procedures require fast and highly reliable segmentation of the pathological regions prior to the treatments. We presented an expert-supervised segmentation method that achieves this goal. The physician can provide feedback regarding the results of a first phase fully-automatic segmentation. The feedback, in the form of a few mouse clicks, is integrated in subsequent phases of the segmentation process. The extension of the current framework to 3D is straightforward. The feedback points can be placed on sagittal, coronal and transverse sections of the initial 3D segmentation. The 3D segmentation processes can be carried out using the same methodology, with 3D rather then 2D coordinate system. This is a subject of a future research.

The experiments are in the context of MRI-guided focused-ultrasound ablation of uterine fibroids. With minimal expert interaction, the segmentation accuracy levels (99.9% true positive fraction and 0.06% false positive fraction), are practically identical to fully-manual expert segmentation. Thus, by providing an intuitive and efficient interaction mechanism, the proposed method allows current image therapy systems to exploit state of the art image segmentation procedures.

6. REFERENCES

[1] T. McInerney and D. Terzopoulos, "Deformable models in medical image analysis: a survey," *Medical Image Analysis*,

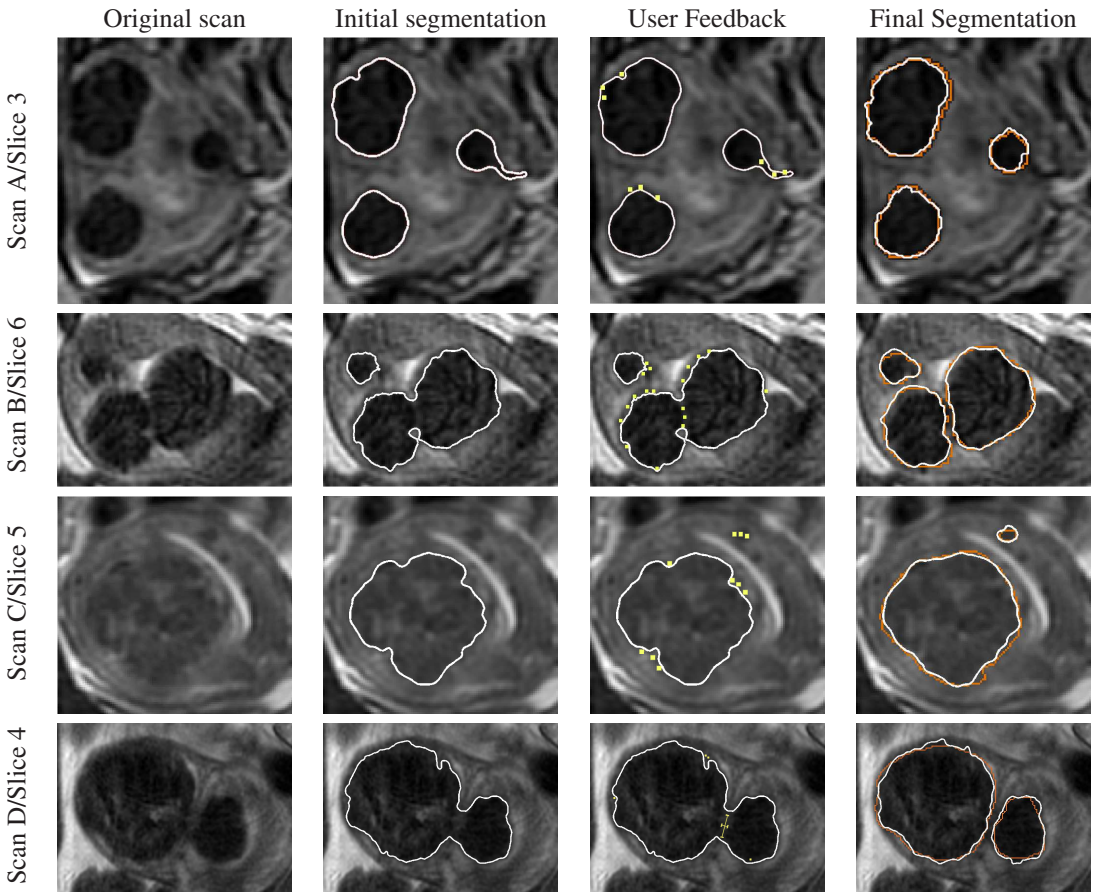

Fig. 1. Segmentations of uterine fibroids in abdomen MR scans of different patients . The last row demonstrates the 'cross mode'. Manual segmentation is shown in red. Quantitative comparison with manual segmentations for the respective images is presented in Table 1.

vol. 1, no. 2, pp. 91–108, 1996.

[2] J. Liang, T. McInerney, and D. Terzopoulos, "United snakes," *Medical Image Analysis*, vol. 10, no. 2, pp. 215–233, 2006.

[3] M. Kass, A.P. Witkin, and D. Terzopoulos, "Snakes: Active contour models," *IJCV*, vol. 1, no. 4, pp. 321–331, 1988.

[4] C. Rother, V. Kolmogorov, and A. Blake, "Grabcut: Interactive foreground extraction using iterated graph cuts," *SIGGRAPH*, 2004.

[5] A. Protiere and G. Sapiro, "Interactive image segmentation via adaptive weighted distances," *Trans. Imag. Proc.*, vol. 16, no. 4, pp. 1046–1057, 2007.

[6] A. Falcao *et. al.*, "User-steered image segmentation paradigms - live wire and live lane," *Graph. Models and Image Proc.*, vol. 60, no. 4, pp. 233–260, 1998.

[7] E. N. Mortensen and W. A. Barrett, "Interactive segmentation with intelligent scissors," *Graph. Models and Image Proc.*, vol. 60, no. 5, pp. 349–384, 1998.

[8] N. Paragios, "Variational methods and partial differential equations in cardiac image analysis," *ISBI*, vol. 1, pp. 17–20, 2004.

[9] H. Li, A. Yezzi, and L.D. Cohen, "3D brain segmentation using dual-front active contours with optional user interaction," *Intl. J. of Biomedical Imaging*, pp. 1–17, 2006.

[10] D. Cremers *et. al.*, "A probabilistic level set formulation for interactive organ segmentation," in *Proc. of the SPIE Medical Imaging*, 2007.

[11] S. Osher and J.A. Sethian, "Fronts propagating with curvature-dependent speed: Algorithms based on Hamilton-Jacobi formulations," *J. of Comp. Physics*, vol. 79, pp. 12–49, 1988.

[12] T.F. Chan and L.A. Vese, "Active contours without edges," *Trans. Image. Proc.*, vol. 10, no. 2, pp. 266–277, 2001.

[13] V. Caselles, R. Kimmel, and G. Sapiro, "Geodesic active contours," *IJCV*, vol. 22, no. 1, pp. 61–79, 1997.

[14] S. Kichenassamy *et. al.*, "Gradient flows and geometric active contour models," in *ICCV*, 1995, pp. 810–815.

[15] A. Fenster and B. Chiu, "Evaluation of segmentation algorithms for medical imaging," *Eng. in Medicine and Biology*, pp. 7186 – 7189, 2005.

[16] N. Ben-Zadok, T. Riklin Raviv, and N. Kiryati, "Interactive level set segmentation for image-guided therapy: Examples," http://www.eng.tau.ac.il/~nk/ISBI09/, 2009.